Association of Metallurgical Engineers Serbia and Montenegro *Scientific paper*
AME *UDC:669.14.018.001.972:620.17=861*

AME MODELLING THE MECHANICAL BEHAVIOUR OF STEELS WITH MIXED MICROSTRUCTURES

I. GUTIERREZ

CEIT and Tecnun (University of Navarra),
Manuel de Lardizábal 15, 20018 San Sebastián, Spain

ABSTRACT

The present work describes the methodology that has been followed in order to model the flow curves for mixed steel microstructures. As a first stage, a physically based model has been developed in order to predict the mechanical behaviour of different steel micro-constituents. Nan hardness tests have been used in order to check the accuracy of such predictions when applied to each micro-constituent in the mixed microstructure. An auto consistent model has been feed with such formulas and applied to mixed microstructures. The results have been checked against tensile curves and the experimental determination of the strain partitioning allowed investigating the validity of the predictions.

Key words: steels, ferrite, pearlite, martensite, tensile, nanohardness, mixed microstructures, dual phase, strain partitioning, modelling

INTRODUCTION

The coupled combination of chemical composition and processing conditions is able to produce in steels a broad range of microstructures of significantly different mechanical behaviour. Most commonly, ferrite-pearlite, have been extensively applied in low carbon strips and structural steels for a broad range of applications requiring, depending on the application, moderate strength, good toughness, weldability and formability, among others. The increasing demand by the market of steel products with enhanced mechanical behaviour has lead to the extension of the range of microstructures being produced in strip and sections.

In order to reach property combinations beyond the limit achievable with more conventional microstructures, higher complexity ones are progressively put into production. The direct consequence is that the determination of the relations between the microstructure and the mechanical behaviour becomes a problem of increasing complexity. Most of the equations already available in the literature for steel microstructures relate the yield stress or the tensile strength to the steel composition and to a series of variables related to the microstructure [1]. The prediction of the flow curve is mainly based on empirical formulations like the Ludvik-Hollomon equation and its variants. Such a formulation has mainly been applied for ferrite, but some expressions can also be found for other steel microstructures [2, 3, 4].

In a mixed microstructure formed by more than one micro-constituent, it is very often considered that the yield stress can be defined by the sum of the yield stress of each of the components weighted by its volume fraction. However, this quite simplistic approach gives very often significant deviations form experiment and is not able to

describe plasticity. The development of models for mixed microstructures requires more elaborated formulations [5]. The present work describes the methodology that has been followed in order to model the flow curves for mixed steel microstructures using physically based equations to predict the mechanical behaviour of each of its micro-constituents.

THE RULE OF MIXTURES

For materials being constituted by two or more phases, the modified rule of mixtures [5] can be used as an homogenisation technique:

$$\sigma_{Mix} = f_1 \sigma_1 + (1-f_1) \sigma_2 \quad (1)$$

$$\varepsilon_{Mix} = f_1 \varepsilon_1 + (1-f_1) \varepsilon_2 \quad (2)$$

with σ_{Mix} and ε_{Mix} being respectively the stress and the strain of the material and f_i , σ_i and ε_i, the volume fraction, stress and strain of each one of its components.

The Eq. 1 and 2 that can be considered as upper and lower bounds [6] are frequently taken separately assuming iso-strain or iso-stress. However, when the strength of both phases is significantly different these simplifications lead to predictions that are far from being accurate. The best known example affects ferrite-pearlite microstructures. Both micro-constituents have significantly different yield stresses, but an empirical equation has been proposed [7]:

$$\sigma = (1 - f_p^{\,n})\sigma_\alpha + f_p^{\,n}\sigma_p \quad (3)$$

which is a modification of Eq. (1), in order to correct for the discrepancies with experiment when considering iso-strain. This empirical equation avoids for this particular case the complex resolution of the system defined by Eqs (1) and (2).

STRAIN PARTITIONING

Experimental evidence can be found showing that, in mixed microstructures, the strain does not distribute homogeneously between the micro-constituents [8,9, 10]. The strain partitioning has been determined from microstructure in ferrite-pearlite and in ferrite-martensite tensile specimens [9]. The micrograph sequences in Figs. 1 and 2 show the evolution of the mixed microstructures during the tensile tests. The ferrite is observed to deform preferentially when being together with a harder micro-constituent like pearlite or martensite. This is better appreciated in Fig. 3 in which the plastic strain in each of the micro-constituents has been plotted as a function of the macroscopic plastic strain in the specimen for ferrite-pearlite and ferrite-martensite microstructures. Pearlite enters plasticity, but in a significantly lower proportion than does ferrite. The main differences are observed for the 0.3%C steel in which case the volume fraction of pearlite reaches about 60%. The strain ratio slightly decreases for lower carbon content (0.15% C) and volume fraction of pearlite (30%).

For the ferrite-martensite combinations, martensite is not observed to deform plastically to a significant extent before necking. This is a quite common behaviour due to a high stress ratio between ferrite and martensite. Most of the plastic deformation concentrates in ferrite and at increasing macroscopic strains, unless the internal stresses can be relaxed by the plastic deformation of the martensite, the plastic incompatibility leads to the formation of cracks like those, in the example shown in Fig. 4, affecting some interfaces located perpendicular to the tensile axis.

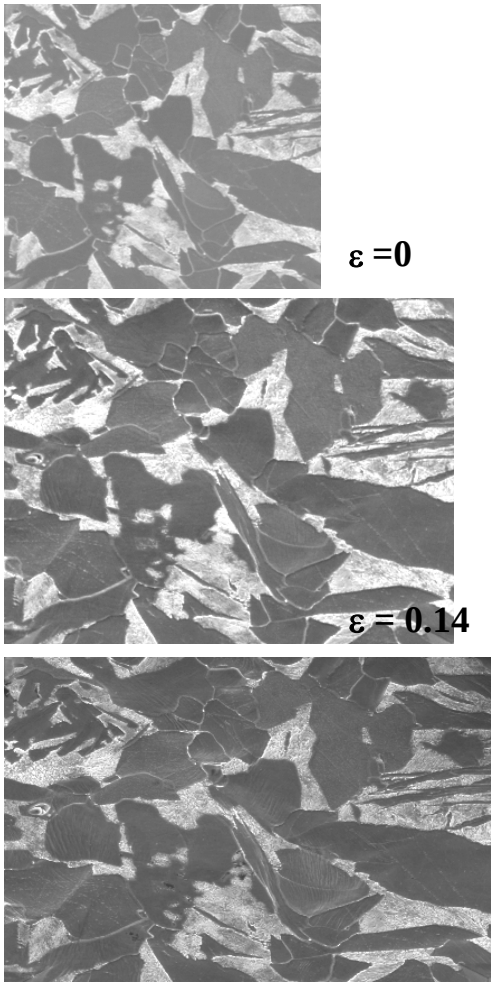

Fig. 1. Evolution, with the macroscopic plastic strain, of a ferrite (dark) pearlite (light) microstructure [9]

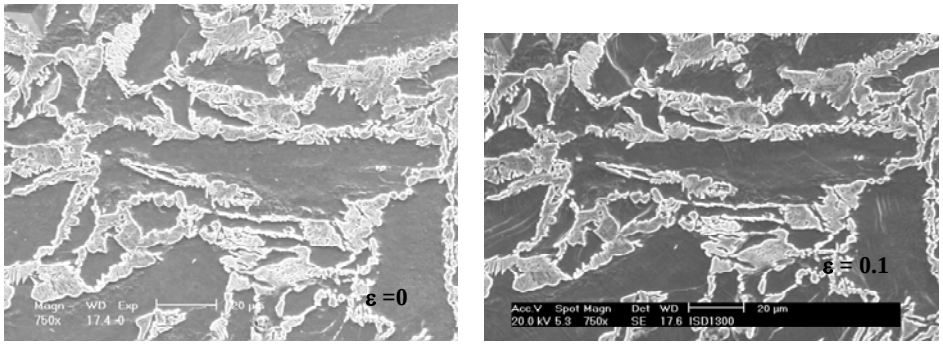

Fig. 2. Evolution, with the macroscopic plastic strain, of a ferrite (dark) martensite (light) microstructure [9]

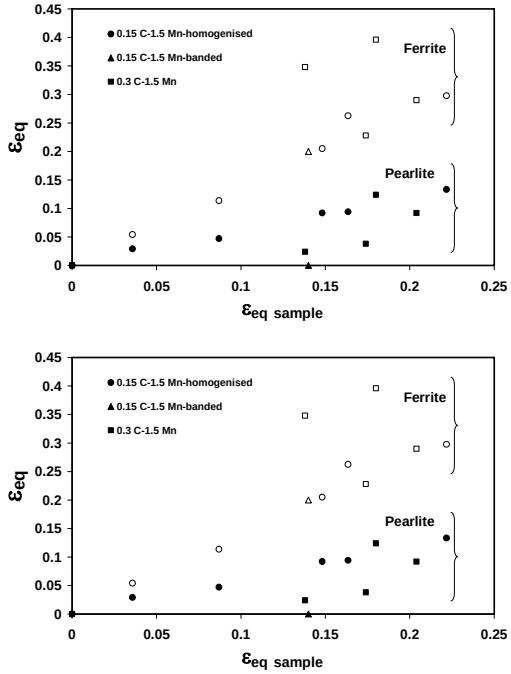

Fig. 3. Experimental true plastic strain partitioning for ferrite-pearlite and ferrite-martensite microstructures [9]

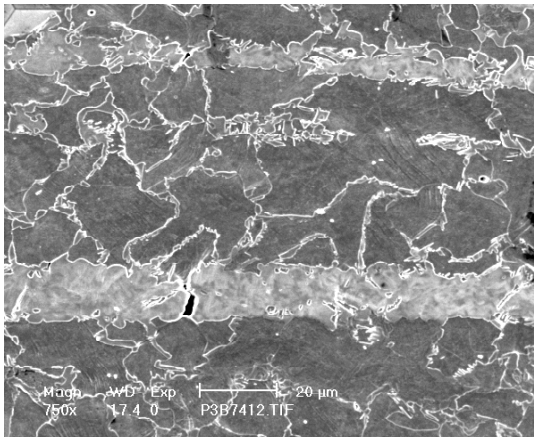

Fig. 4. Cracks almost perpendicular to the tensile axis, formed in martensite bands at high macroscopic strains [9]. Ferrite (dark) martensite (light).

Implementation of the models. The above results clearly show the inaccuracy of assuming iso-strain. Different approaches have been developed to solve analytically or by finite elements (FE) the system of equations defined by Eq. 1 and 2. The simplest approach is to use an arbitrary fitting parameter [5, 11]:

$$q = \frac{\sigma_1 - \sigma_2}{\varepsilon_1 - \varepsilon_2} \qquad (4)$$

But other methods have also been used like the imposition of a given set of conditions like the macroscopic strain energy being an extreme [12] or the equality of the mechanical work increment in each micro-constituent [13].

Micromechanics, has also been applied that needs to solve the questions related to the matrix-disperse phase interaction and the interaction between the dispersoids. To answer to the first of these questions, self consistent models [14, 15] have been build up on the base of Eshelby inclusion theory [16]. The concept of the secant moduli [17] allows introducing into a relatively simple mathematical formulation the weakening constrain power of the matrix due to its plastic relaxation around the hard particles. The interaction between the disperse particles is best described through Mori-Tanaka [18] mean field approach.

Most of the resultant models being currently used follow the method proposed by Tomota and coworkers [19] and divide the deformation range into three different stages:

Stage I: Both phases deform elastically.

Stage II: The soft phase deforms plastically and the hard one elastically.

Stage III: Both phases deform plastically.

Based on the secant moduli method, together with the Eshelby and mean field formulations, Weng [20] has developed a model applicable to two phase ductile materials. This new approach has been successfully applied to model the tensile curves in dual multiphase steels [21] and will be used here.

The above models require the knowledge of the stress-strain behaviour of each micro-constituent into the mixed microstructure.

FLOW CURVES FOR EACH MICRO-CONSTITUENT

Empirical approach: The application of the above formulations for mixed microstructures requires, independently of the selected approach, the previous development of equations describing, as accurately as possible, the mechanical behaviour (stress-strain curve) for each micro-constituent. The most popular formulation based on empirical equations is the Ludvik-Hollomon equation:

$$\sigma = K_o \, \varepsilon^n \qquad (5)$$

or some modifications of it, as for example the Swift-Griffits equation:

$$\sigma = K \, (\varepsilon + \varepsilon o)^m \qquad (6)$$

the limitation of these models is the reduced applicability, as they are based on fitted parameters that cannot easily be extrapolated to other conditions. For ferrite this has been overcome to a certain level relating the exponent n to the grain size [22] and to composition [2]. However, when the degree of complexity of the steel microstructure increases, the applicability of these empirical equations reduces. In some cases, the use of different n values is required in order to fit the flow curve over the entire deformation range [23].

Physically based models: An alternative to the empirical equations is the use of physically based models that link the micro and the macro scales and are expected to give more accurate results. Different dislocation based models can be found that have some differences in the formulation but all of them relate the strain hardening to the balance between the dislocation storage and recovery.

The macroscopic flow stress, σ, and the plastic strain, ε, are related to the critical resolved shear stress for current microstructure state, τ, and amount of crystallographic

slip, γ, via an orientation factor, M as: σ = Mτ and M.dε = dγ. Assuming an average behaviour, the microscopic hardening rate of the crystalline element, θ = dτ/dγ can be related to the macroscopic hardening as [24]:

$$\theta = M^{-2}\frac{d\sigma}{d\varepsilon}. \qquad (7)$$

The classical relation between the flow stress and the total dislocation density is:

$$\sigma = \sigma_o + \Delta\sigma_\varepsilon = \sigma_o + \alpha M \mu b \sqrt{\rho} \qquad (8)$$

with α a constant, M the Taylor factor, μ the shear modulus, b the Burgers vector and ρ the dislocation density.

During deformation, the evolution of the dislocation density with strain is generally considered to depend on two terms [25]:

$$\frac{d\rho}{d\gamma} = \left.\frac{d\rho}{d\gamma}\right|_{stored} - \left.\frac{d\rho}{d\gamma}\right|_{recovery} \qquad (9)$$

The substitution of M.dε = dγ allows expressing the change in dislocation density as a function of the macroscopic equivalent strain, ε. Different expressions have been deduced to express each term. Frequently [25,26], it is considered that:

$$\frac{d\rho}{d\varepsilon} = M\left(\frac{1}{bL} - k_2\rho\right) \qquad (10)$$

with k_2 a constant and L the dislocation mean free path. L can be expressed as being proportional to the average spacing of the homogeneously distributed dislocations, $\rho^{-1/2}$, or can alternatively be defined by some microstructural parameter like the subgrain size, the interparticle spacing or the grain size. The resulting equations and the results of the integration, considering ρ_o as being the initial dislocation density in the deformation free material give different results, depending on the chosen option [27]. After integration and substitution into Eq. 8, it results [9]:

L = constant	$\rho = \frac{1}{bLk_2}\left[1-\exp(-k_2M\varepsilon)\right] + \rho_0\exp(-k_2M\varepsilon)$ (11)
	$\Delta\sigma_\varepsilon = \alpha M\mu b\left[\frac{1}{bLk_2}\left[1-\exp(-k_2M\varepsilon)\right] + \rho_0\exp(-k_2M\varepsilon)\right]^{0.5}$ (12)
$L = \frac{1}{k_1\sqrt{\rho}}$	$\rho = \frac{k_1}{k_2}\left[1-\left(1-\frac{k_2b}{k_1}\sqrt{\rho_o}\right)\exp(-\frac{k_2M\varepsilon}{2})\right]$ (13)
	$\Delta\sigma_\varepsilon = \alpha M\mu\frac{k_1}{k_2}\left[1-\left(1-\frac{k_2b}{k_1}\sqrt{\rho_o}\right)\exp(-\frac{k_2M\varepsilon}{2})\right]$ (14)

The above formulation has been applied in order to predict the tensile curves for different steel micro-constituents. The application of these equations to the experimentally determined tensile curves requires some fitting exercise to determine the involved parameters. The practical result is that, independently of the approach being used, it is possible to predict with enough precision the tensile curve, by the correct selection of the parameters. In the work described here, care has been taken to relate the

different parameters involved into the equations to the main characteristics of each particular microstructure.

For ferrite, given that the initial dislocation density before deformation is low, the following equation can be applied [9, 28, 29]:

$$\sigma = \sigma_o + \alpha M \mu \sqrt{b} \sqrt{\frac{1-\exp(-Mk_2\varepsilon)}{k_2 L}} \qquad (15)$$

which is a simplified version of Eq. (12). In this equation, ε is the plastic strain, μ=80000MPa and b=2.5 10^{-10} m. There is some uncertainty concerning the value of α´= αM to be used. For the case of ferrite, factors of variation as high as 1.8 can be found between the α´ values reported by different authors, see Ref. [3]. This strongly affects the strain hardening contribution to the overall result of the modelling. In the present case, α=0.33 and M=3 have been fixed for the different microstructures and consequently remain out of the required fitting exercise to the experimental tensile curves. The term σ_o has been taken the same than that reported by other authors to describe the effect of the Peierls stress and of the elements in solid solution [28]:

$$\sigma_o = 77 + 80\%Mn + 750\%P + 60\%Si + 80\%Cu + 45\%Ni + 60\%Cr + 11\%Mo + 5000(N_{ss}+C_{ss}) \qquad (16)$$

L has been replaced by the ferrite grain size expressed by the mean linear intercept, d_α and the values of k_2 that have been obtained by fitting have been found to depend inversely on d_α, leading to:

$$k_2 = \frac{10^{-5}}{d_\alpha} \quad (d_\alpha \text{ in } m) \qquad (17)$$

For pearlite, it is generally accepted that the strain hardening is controlled by the dislocation density in ferrite. Dollar et al. [3] have determined experimentally the dislocation density in the pearlitic ferrite, as a function of the plastic macrospocic strain, Fig. 5. A constant mean free path has also been assumed for the plastic deformation of pearlite and consequently, Eq. (11) has been applied. As can be seen in the figure, a reasonable agreement can be reached between the predictions of model and the experimental dislocation density when a value L = 2 10^{-6} m and k_2 = 7 are substituted into Eq. (11). The required value of L that, according to the previous hypothesis, represents the dislocation mean free path is about one order of magnitude larger than the interlamellar spacing. However, the obtained result seem in agreement with experimental results obtained for pearlitic steels [3] suggesting that the strain hardening is independent of the interlamellar spacing.

This value of L has been substituted into the following equation:

$$\sigma = \sigma_o + 3\,\mu\, b\, \lambda^{-1} + f\alpha M \mu \sqrt{b} \sqrt{\frac{1-\exp(-Mk_2\varepsilon)}{k_2 L}} \qquad (18)$$

which is a modification of Eq. (15) in order to predict the tensile curves for pure pearlitic steel microstructures. The second term takes into account the contribution of the interlamellar spacing, λ, to the yield stress [3]. The factor *f* adopts a value close of 2 for eutectoid compositions and decreases to 1, as the carbon content of the pearlite decreases.

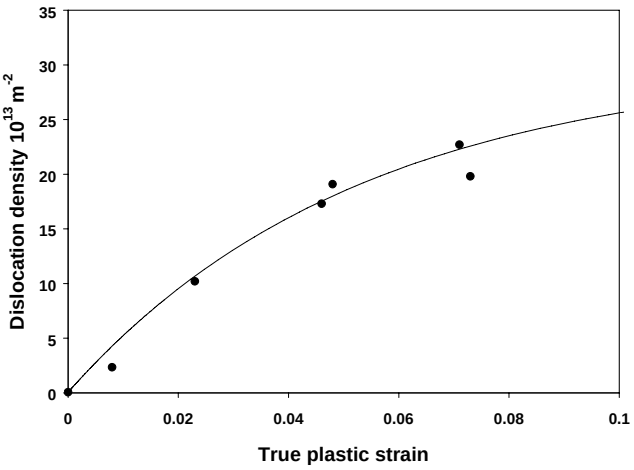

Fig. 5. Dislocation density in the ferrite, as a function of the true plastic strain in pearlitic steel. The points are experimental data from Ref. 3. The line corresponds to the predictions from Eq. 11

For martensite, the above formulation applied for ferrite and for pearlite, using L constant can also be applied to describe the experimental curves. However, the value of $L = 3.8\ 10^{-8}$ m that allows getting a reasonable agreement with the experimental tensile curves is one order of magnitude lower than the width of laths to which presumably could be associated the dislocation mean free path [29]. This indicates that, for martensite, in spite of getting a reasonable agreement in terms of fitting, the hypothesis made based on a constant L does not seem to be the most appropriate. Taking into account that as quenched martensites contain a high density of transformation dislocations, it could be assumed L relates to the dislocation spacing. Accordingly, an alternative approach, based on Eq. 14, has been applied [30] together with:

$$log(\rho_o) = 8.9372 + \frac{6880.93}{T} - \frac{1780360}{T^2} \qquad (19)$$

and

$$k_1 = (1.69\ 10^{-7}\ \sqrt{\rho_o}\ - 4.52) \qquad (20)$$

with $T = M_s$ the martensite start temperature. These equations have been determined by fitting. The first of them represents the transformation dislocation density in martensite and is similar to that previously reported by other authors [31], but leads to a density about 45% lower. The same type of formulation also agrees for bainite (with T the isothermal transformation temperature) by slightly modifying the transformation dislocation density and the coefficients relating k_1 to ρ_o.

Given that the application of the physically based model is made on the base of tensile curves, it is not possible to extract conclusions about the exact mechanism controlling the strain hardening. However, according to the described results, Eq. 14 seems to apply reasonably well to bainite and martensite single component microstructures, while Eq. 12 gives reasonable results for ferrite and for pearlite.

Predictions from nanohardness test: The above formulation has demonstrated to produce consistent results for single constituent microstructures. However, when applied

to predict the mechanical behaviour of each micro-constituent in a mixed microstructure some questions can be addressed about its predictive accuracy. The main discrepancy is expected to come from the elements partitioning during the phase transformation leading to the production of the microstructure and also from the interactions between the phases. Nanohardness can be used [9] as a tool to investigate the accuracy of the predictions. In a fine multi-constituent microstructure, small indentation depths need to be selected in order to avoid interaction in the measurements coming from the neighbourhood. However, it has to be taken into account that size effects strongly affect the results at small indentation depths [32]. Nanoindentations carried out at different imposed depths on Cu, Al and steels with different compositions and microstructures allowed deducing empirical linear relationships relating the obtained values for nanohardness to the 0.2% proof stress, σ_y, and the maximum uniform stress, σ_u, [32].

$$\sigma_y = \frac{0.25H}{\sqrt{1+\frac{0.3}{h}}} \tag{21}$$

$$\sigma_u = \frac{0.34H}{\sqrt{1+\frac{0.3}{h}}} \tag{22}$$

with H the nanohardness in MPa and h the indentation depth in μm. These relations are applicable for $h \geq 0.25$ μm. For smaller indentation depths, the results deviate from this relation probably due to some limitations of the theory proposed by Nix and Gao [33] that is the base for the above equations.

The results in Fig. 6 show the variation of nanohardness with the carbon content in martensite [9, 34]. Some of the data correspond to martensite in ferrite-martensite (F+M) microstructures, while the rest belong to fully as quenched martensitic samples. The general expected trend, with hardness increasing with the carbon content, is observed.

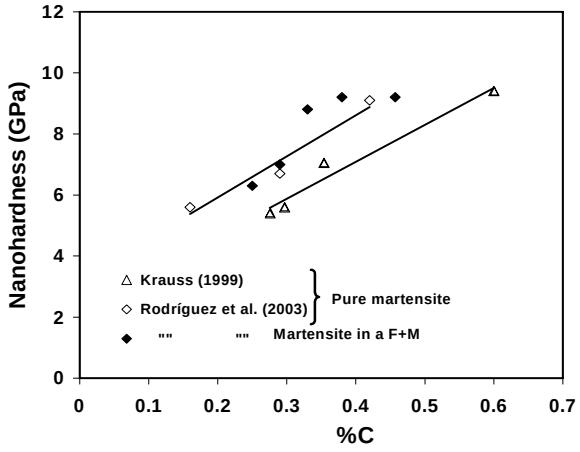

Fig. 6. Nanohardness as a function of the carbon content in martensite in mixed microstructures (estimated) and in pure martensite [9, 34]. The data in Ref. [9] were obtained for a 0.25 μm indentation depth

The nanohardness in ferrite is systematically higher for F+M microstructures than in ferrite-pearlite ones. Some intercritical treatments have been performed at a

temperature of 730ºC in order to transform pearlite into austenite and revert this last to martensite during the subsequent water quenching. The results in Fig. 7, clearly show that the ferrite in the ferrite-martensite microstructure is harder by an amount ΔH, than that in a ferrite-pearlite microstructure. Some increase of the carbon in solution in ferrite in the quenched material can be one of the factors that contribute to such strengthening, but the most important contribution probably comes from the deformation of the ferrite in the vicinity of the martensite islands. In fact, the formation of martensite involves an increase of volume [35]:

$$\frac{V_M}{V_\alpha} = 1 + 0.045\%C \qquad (23)$$

that is considered as being the responsible of the dislocation density increase in the neighbouring ferrite [36, 37].

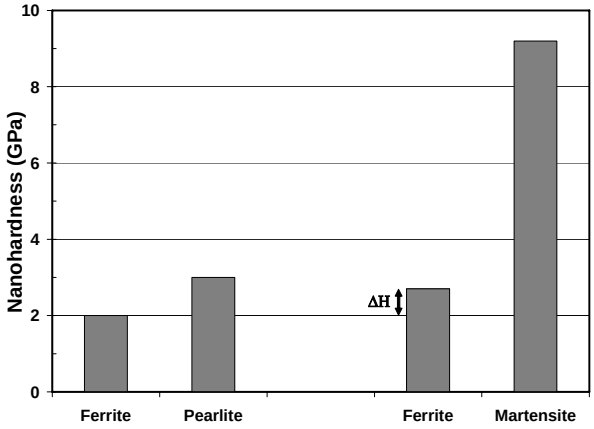

Fig. 7. Nanohardness in the microstructural constituents for a ferrite-pearlite and for pearlite-martensite microstructures [9]

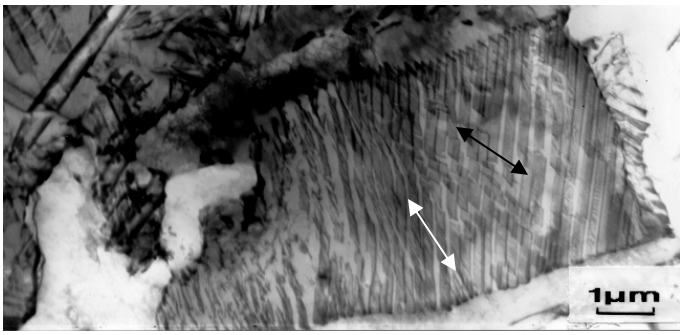

Fig. 8. Shearing in pearlite, produced by the formation of bainite/martensite in its neighbourhood [9].

In agreement with this, transmission electron microscopy (TEM) observations made on ultra-fast quenched samples show that the formation of bainite/martensite at a latter stage of the transformation, produces some straining on previous phases formed at

higher temperatures [9]. An example of this in shown in Fig. 8. The formation of bainite and martensite has produced the shearing of the cementite lamellae of the previously formed pearlite.

PREDICTION OF THE TENSILE CURVES FOR MIXED MICROSTRUCTURES

The model proposed by Weng [20] has been finally applied in order to predict the tensile curves for ferrite-pearlite and for ferrite-martensite microstructures [9]. This model assumes both phases can undergo plastic flow and applies the Hill´s [15] matrix weakening constraint for the case in which the matrix is the softest phase. In the present case, the ferrite, which is the softest micro-constituent in the different analysed microstructures is matrix and accordingly such approach seems the adequate. The schematic representation in Fig. 9 shows the distribution of strain and stress on the soft and hard micro-constituents and in the mixed microstructure for a given macroscopic strain. The slopes of the straight lines represent the respective secant Young moduli. When applying Weng´s model, the three different deformation stages proposed by Tomota et al. [19] and mentioned above, need to be considered.

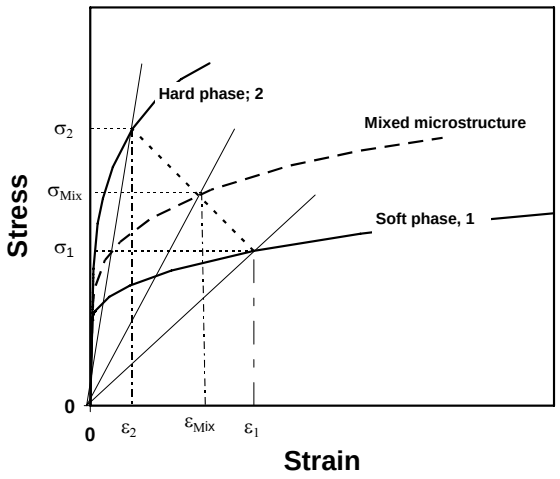

Fig. 9. Schematic representation of the secant Young´s modulus method applied to the stress-strain curves of the micro-constituents and of the mixed microstructure.

It can be seen, Fig. 10, that a reasonable agreement is obtained between the predictions of the model and the experimental curves for different ferrite-pearlite microstructures when the tensile curve for each microconstituent is estimated from the physically based model described above. However, for ferrite-martensite microstructures, the equation for the ferrite needs to be modified in order to take into account the strengthening produced by the martensite formation. An empirical approach has been applied, as a first approximation. This considers an effective dislocation mean free path in ferrite, L_{eff}, being lower than the grain size [10]:

$$L_{eff} = C\, d_{\alpha} \qquad (24)$$

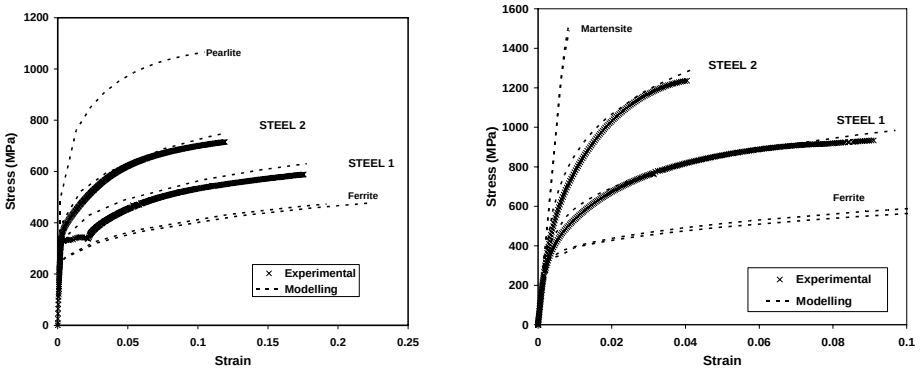

	C	Si	Mn	P	N	Pearlite in F-P (%)	Martensite in F-M (%)
Steel 1	0.16	0.25	1.50	0.012	0.0084	31	42
Steel 2	0.29	0.26	1.50	0.011	0.0076	61	76

Fig. 10. Experimental and predicted curves a) ferrite pearlite and b) ferrite martensite. Steel composition and volume fraction of the microstructural constituents in ferrite-pearlite and in ferrite-martensite microstructures [9]

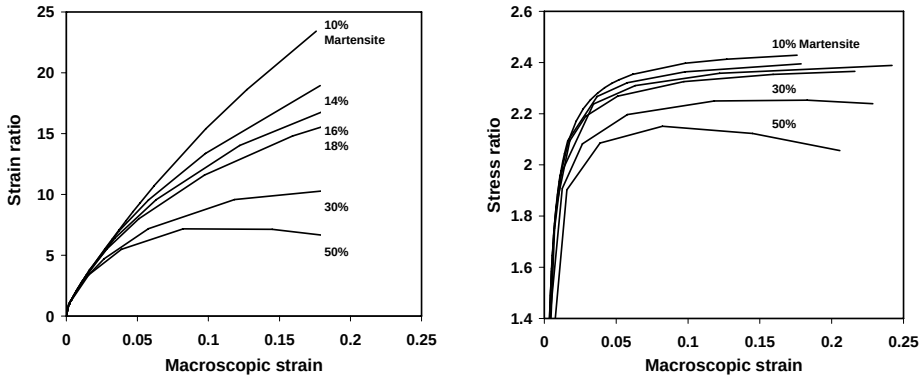

Fig. 11. Predicted strain and stress ratios for ferrite-martensite microstructures, according to Weng´s model

A reasonable agreement has been obtained taking a value for C of 0.6, but further developments are required in order to get a more fundamental formulation to describe such effect. Additionally, good agreement is found between the strain partitioning predicted from the model and the experimentally measured strain in the different micro-constituents, Fig. 3.

The curves in Fig. 11, show the ratio between the strain and stress in ferrite and those in martensite, obtained from the model for a given steel and different martensite contents. It can be seen that the decrease in martensite leads to higher ratios both in strain and in stress due to the strengthening of the martensite, as a consequence of its higher carbon content. As a consequence, the plasticity of the martensite progressively decreases.

CONCLUSIONS

- It has been demonstrated that it is possible to apply a physically based formulation to model the tensile curves of different microstructures produced in steels. The parameters involved in such formulation can be related to each particular microstructure characteristics.
- The single constituent model can be applied to predict the mechanical behaviour of each constituent in a mixed microstructure. For ferrite-martensite steels the effect of the strengthening on the ferrite produced by the formation of the martensite needs to be considered.
- An autoconsistent model has demonstrated to agree well with experiment the predicted strain partitioning is well described, which is an additional indication supporting the validity of the model.

ACKNOWLEDGEMENTS

Most part of this work has been carried out with a financial grant from the Research Fund for Coal and steel of the European Community and the CICYT of Spain.

REFERENCES

[1] F.B. Pickering, Structure-Property Relationships in Steels , Materials Science and Engineering, 7,. Ed. Cahn et al., (1993) 45.

[2] Y. Tomota et al., ISIJ, 32 (1992) 343.

[3] M. Dollar et al., Acta Metallurgica, 36, (1988), 311.

[4] P. Buesler., ECSC Steel RTD first report, CECA 7210-PR-044, (1999).

[5] H. Fischmeister, B. Karlsson, Z. Metallkde, 68 (1977) 311.

[6] R. Hill, J. Mech. Phys. Solids, 11 (1963) 357.

[7] T. Gladman, I.D. McIvor, F.B. Pickering, JISI, 210 (1972) 916.

[8] N.K. Ballinger and T. Gladman, Work hardening of dual-phase steels, Metal Science, (1981) 95.

[9] R. Rodriguez and I. Gutierrez in S.V. Parker et al: 'Property Models for Mixed Microstructures', ECSC Agreement no. 7210-PR/166, Final Report, EUR 20880, (2003).

[10]R. Rodriguez, I. Gutierrez, Proc. TMP´2004, Ed. M. Lamberigts, Verlag Stahleisen GMBH, Düsseldorf, (2004) 356.

[11]. S. Sangal, N.G. Goel and K. Tangri, Metall. Trans. A, 16 (1985) 2023.

[12] T.S. Byun, I.S Kim, J. Mater. Sci., 26 (1991) 3917.

[13]. O. Bouaziz and P. Buessler, CIT-La Revue de Metallurgie, 99 (2002) 71.

[14] E. Kröner, Acta metal., 9 (1961) 155.

[15] R. Hill, J. Mech. Phys. Solids, 13 (1965) 89.

[16] J.D. Eshelby, Proc. R. Soc. London, A241, (1957) 376.

[17] M. Berveiler and A. Zaoui, J. Mech. Phys. Solids, 26 (1978) 325.

[18] T. Mori and K. Tanaka, Acta met., 21 (1973) 571.

[19] Y. Tomota, K. Kuroki, T. Mori and I. Tamura," Mater. Sci. Eng., 24 (1976) 85.

[20] G.J. Weng, J. Mech. Phys. Solids, 38 (1990) 419.

[21] Rudiono and Y. Tomota, Acta mater., 45 (1997) 1923.

[22] W.B. Morrisson, Trans. ASTM, 59 (1966) 824.

[23] R.G. Strinfellow, D.M. Parks, Int. J. of Plasticity, 7 (1991) 529.

[24] J. Gil-Sevillano, Materials Science and Technology, Ed. R.W. Cahn et al., 6, (1993), 19.

[25] Y. Bergström, Mat. Sc. Eng. (1969) 193.

[26] Y. Estrin, H. Mecking, Acta Met. 32 (1984) 57.

[27] G. Ferron, E.L. Ouakdi, J.R. Klepaczko and M. Mliha-Touati, Proc. 8th Riso International Symposium, Eds. S.I. Andersen et al., Denmark, (1987) 311.

[28] O. Bouaziz, G. Herman, M. Piette, T. Iung and Ch. Perdrix, "Proc. Thermomechanical Processing of steels Conf., IOM, London, (2000), 342.

[29] R. Rodríguez and I. Gutierrez, Materials Science Forum, 426-432 (2003) 4525.

[30] I. Gutierrez et al. Mechanical property models for high strength complex microstructures, European Commission RFCS Programme, RFCS-PR-02013, Mid term Report, (2005)

[31] C.H. Young, H.K.D.H. Bhadeshia, Mater. Sci. Technol., 10, (1994), 209.

[32] R. Rodríguez and I. Gutiérrez, Mat. Sci. and Eng. A, A361 (2003) 377.

[33] W.D. Nix and J. Gao, J. Mech. Phys. Solids, 46 (1998) 411.

[34] G. Krauss, Mat. Science and Engineering, A 273-275, (1999) 40.

[35] E.C. Bain, H.W. Paxton, Les éléments d´addition dans l´acier, Dunod, Paris, (1968) 36.

[36] G. Tither and M. Lavite, J. Metals, 27 (1975) 15.

[37] U. Liedl, S. Traint and E. A. Werner, Computational Materials Science, 25 (2002) 122.